

Vortex Dynamics in Ferromagnetic Superconductors: Vortex Clusters, Domain Walls and Enhanced Viscosity

Shi-Zeng Lin, Lev N. Bulaevskii and Cristian D. Batista

Theoretical Division, Los Alamos National Laboratory, Los Alamos, New Mexico 87545, USA

(Dated: June 12, 2021)

We demonstrate that there is a long-range vortex-vortex attraction in ferromagnetic superconductors due to polarization of the magnetic moments. Vortex clusters are then stabilized in the ground state for low vortex densities. The motion of vortex clusters driven by the Lorentz force excites magnons. This regime becomes unstable at a threshold velocity above which domain walls are generated for slow relaxation of the magnetic moments and the vortex configuration becomes modulated. This dynamics of vortices and magnetic moments can be probed by transport measurements.

PACS numbers: 74.25.Uv, 74.25.F-, 74.25.Ha, 74.25.N-, 75.60.Ch

Introduction – Superconductivity (SC) and magnetism are at the heart of modern condensed matter physics. While they seem to be antagonist according to the standard BCS theory, a large family of magnetic superconductors were discovered in the last decades. Examples include coexistence of antiferromagnetism or helical ferromagnetic (FM) order in ternary superconducting compounds[1], uniform ferromagnetism in triplet superconductors[2–4], and antiferromagnetism in the $\text{ReNi}_2\text{B}_2\text{C}$ borocarbides[5] (Re represents a rare earth element) and in the recently discovered iron-based superconductors[6]. The interplay between SC and magnetism allows to control the superconducting properties through the magnetic subsystem, and vice versa. These phenomena open new possibilities for applications to superconducting electronics and magnetic storage devices[7, 8].

The Abrikosov vortices of superconductors are a natural link between the superconducting condensate and the magnetic moments. Vortices are induced either by external magnetic fields or by the MMs [9]. On the other hand, the magnetic subsystem supports collective spin-waves and topological excitations that are domain walls. Because vortices are magnetic objects, they are expected to interact strongly with MMs via Zeeman coupling. Indeed, as we discuss below, vortex motion can drive magnetic domain walls.

The MMs provide a novel handle to control the vortex behavior in the static and dynamic regimes. It was demonstrated that magnetic domains induce a vortex pinning that is 100 times stronger than the one induced by columnar defects[10]. In the flux flow regime, vortex motion radiates magnons by transferring energy into the magnetic system. This effect has been recently proposed by Shekhter *et al.* for antiferromagnetic superconductors [11]. By assuming a rigid vortex lattice and fast relaxation of the MMs, it is demonstrated that Cherenkov radiation of magnons occurs when the vortex lattice velocity, \mathbf{v} , satisfies $\mathbf{G} \cdot \mathbf{v} = \Omega(\mathbf{G})$, where \mathbf{G} is the vortex lattice wave vector and $\Omega(\mathbf{G})$ is the magnon dispersion. This emission gives an additional contribution to the vortex viscosity that manifests as a voltage drop in the I-V characteristics. Thus, the overall dissipation is reduced for a given current. Vortex motion can also be used to probe the spectrum of excitations in the magnetic subsystem.[12]

Several questions remain to be addressed. It is known that intrinsic nonlinear effects of the magnetic subsystem become important for high energy magnon excitations. However, it is unclear if magnon excitations remain stable in this nonlinear regime. On the other hand, the interaction between the magnetic subsystem and vortices may become comparable or even stronger than the inter-vortex repulsion. Therefore, the vortex lattice may be modified by this effect. Finally, the dominant dissipation mechanism of vortices when domain walls are excited by the vortex motion is unknown.

Here we study the vortex dynamics in FM superconductors. The Zeeman coupling between vortices and MMs induces an additional vortex-vortex attraction that is comparable to the inter-vortex repulsion for a large enough magnetic susceptibility. This attraction leads to the formation of vortex clusters at low vortex densities. We also show that magnetic domain walls are created when vortex clusters driven by the Lorentz force reach a threshold velocity. The interaction between domain walls and vortices greatly enhances the vortex viscosity and causes hysteresis in the dynamics of the whole system. The vortex configuration is modulated by the domain walls.

Model– Uniform FM order and SC suppress each other because of the exchange and electromagnetic coupling between the MMs and Cooper pairs[1]. However they could coexist in triplet FM superconductors [2–4], such as UGe_2 , layered magnetic superconductors consisting FM and SC layers [13, 14], such as $\text{Sm}_{1.85}\text{Ce}_{0.15}\text{CuO}_4$, or artificial bilayer systems[8, 15]. Here we study the vortex dynamics in these FM superconductors. An applied dc magnetic field perpendicular to the ferromagnetic easy axis creates a vortex lattice that is driven by a dc in-plane current. We use the approximation of straight vortex lines and the description of vortices is two dimensional.

The total Gibbs free energy functional of the system, in terms of the vector potential \mathbf{A} , magnetization \mathbf{M} and vortex position $\mathbf{R}_i = (x_i, y_i)$, is

$$G(\mathbf{A}, \mathbf{M}, \mathbf{R}_i) = d \int dr^2 (g_{\text{sc}} + g_M + g_{\text{int}}) + \frac{1}{8\pi} \int_{\text{out}} dr^3 \mathbf{B}^2, \quad (1)$$

where d is the thickness of the system and the last term is the magnetic energy outside the superconductor. The energy

functional density for the SC subsystem in the London approximation is

$$g_{\text{sc}}(\mathbf{A}) = \frac{\mathbf{B}^2}{8\pi} - \frac{\mathbf{B} \cdot \mathbf{H}_{\text{ext}}}{4\pi} + \frac{1}{8\pi\lambda_L^2} \left(\frac{\Phi_0}{2\pi} \nabla\phi - \mathbf{A} \right)^2, \quad (2)$$

with $\mathbf{B} = \nabla \times \mathbf{A}$. ϕ is the superconducting phase, H_{ext} is the applied magnetic field, λ_L is the London penetration depth and $\Phi_0 = hc/2e$ is the flux quantum. The energy functional density of the magnetic subsystem is

$$g_M = \frac{J}{2} (\nabla \mathbf{M})^2 - \frac{J_A}{2} M_x^2, \quad (3)$$

where J and J_A are the exchange and anisotropy parameters. The easy axis is taken along the x direction. We assume that the magnitude of the magnetic moment is conserved, $|M| = M_s$, where M_s is the saturated magnetization value. Because of the anisotropy, the magnetic Hamiltonian has two degenerate minima and supports stable domain walls. The Zeeman interaction between MMs and SC is

$$g_{\text{int}} = -\mathbf{B} \cdot \mathbf{M}. \quad (4)$$

The vortex axis is taken along the z direction. The straight vortex lines approximation is valid when $d \ll \lambda_L$ or $d \gg \lambda_L$. The spreading of magnetic field associated with vortices near the surface of superconductors has to be taken into account for $d \sim \lambda_L$. [16]. By minimizing $g_{\text{sc}} + g_{\text{int}}$ with respect to \mathbf{A} , we obtain the magnetic field associated with vortices

$$\lambda_L^2 \nabla \times \nabla \times (\mathbf{B} - 4\pi \mathbf{M}) + \mathbf{B} = \Phi_0 \sum_i \delta(\mathbf{r} - \mathbf{R}_i) \hat{\mathbf{z}}. \quad (5)$$

$M_z(k) = B_z(k) \tilde{\chi}_{zz}(k)$ in the linear response region when $M_z/M_s \ll 1$. As λ_L is much larger the magnetic correlation length $\xi_m \sim \sqrt{J/J_A}$, we can use a local approximation for $\tilde{\chi}_{zz}(k) \simeq 1/J_A = \chi_0/(1 + 4\pi\chi_0)$. The uniform susceptibility $\chi_0 \propto \langle M_z(\mathbf{k}=0) M_z(\mathbf{k}=0) \rangle$ diverges at $J_A = 4\pi$, which signals an instability of the magnetic subsystem. The FM ordering along the x -direction coexists with superconductivity only when $J_A > 4\pi$. [17]

According to Eq.(5), the magnetic field of a vortex at \mathbf{R}_i is

$$B_z(\mathbf{k}, \mathbf{R}_i) = \frac{\Phi_0}{1 + \lambda_e^2 \mathbf{k}^2} \exp(i\mathbf{k} \cdot \mathbf{R}_i), \quad (6)$$

with a renormalized penetration depth $\lambda_e \equiv \lambda_L / \sqrt{1 + 4\pi\chi_0}$.

Attraction between vortices via MMs – We calculate now the interaction between two vortices at \mathbf{R}_i and \mathbf{R}_j . Vortices interact with each other through the exchange of massive photons described by g_{sc} , which leads to a short-range repulsion. As was first discussed by Pearl, vortices also interact through the exchange of massless photons outside the SC, as described by the last term in Eq. (1). This contribution leads to a long-range repulsion[18, 19]. The total repulsion energy is

$$U_r(R) = \frac{\Phi_0^2 d}{8\pi^2 \lambda_e^2} K_0 \left(\frac{R}{\lambda_e} \right) + \frac{\Phi_0^2}{8\pi \Lambda} \left[H_0 \left(\frac{R}{\Lambda} \right) - Y_0 \left(\frac{R}{\Lambda} \right) \right], \quad (7)$$

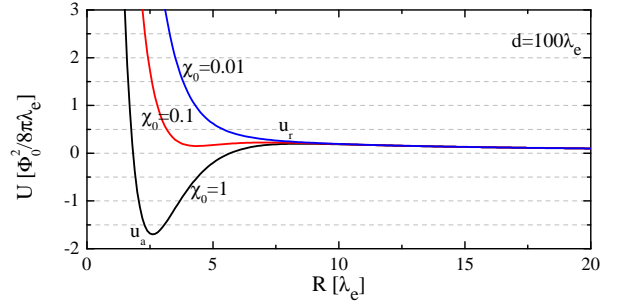


FIG. 1. (color online) Vortex-vortex interaction potential for different values of χ_0 according to Eqs. (7) and (8). Attraction is induced due to the Zeeman coupling between vortices and MMs, and the long-range repulsion arises from the electromagnetic fields outside the SC.

with $\mathbf{R} \equiv \mathbf{R}_i - \mathbf{R}_j$ and $\Lambda = 2\lambda_e \coth[d/\lambda_e]$ is the modified Pearl length. K_1 is the modified Bessel function, H_0 is the Struve function and Y_0 is the Weber function.

A vortex at \mathbf{R}_i polarizes the surrounding MMs. This effect leads to an effective attraction to a vortex at \mathbf{R}_j . The magnetic energy due to the presence of vortices is $d \int dr^2 (g_M + g_{\text{int}})$ with $B_z^v = B_z(R_i) + B_z(R_j)$ and $M_z^v = \chi_0 B_z^v / (1 + 4\pi\chi_0)$. The contribution from the gradient term in Eq. (3) is much smaller than the anisotropic contribution because $k\xi_m \ll 1$ with $k \sim 1/\lambda_e$. By using $M_x^2 + M_z^2 = M_s^2$, we obtain the attractive interaction

$$U_a(R) = -\frac{d}{2} \int dr^2 B_z^v M_z^v = -\frac{d\chi_0 \Phi_0^2 R}{4\pi(1 + 4\pi\chi_0)\lambda_e^3} K_1 \left(\frac{R}{\lambda_e} \right). \quad (8)$$

In the presence of attraction, the repulsion through the electromagnetic fields outside the SC in Eq. (7) cannot be neglected because it prevents the formation of a single cluster. The physics here is similar to the laminar phase in conventional type I superconductors[20].

The effect of finite velocity, \mathbf{v} , on the vortex-vortex interaction is negligible because $\tilde{\chi}_{zz}$ depends weakly on \mathbf{v} for $\xi_m/\lambda_e \ll 1$. The attractive component is comparable to the repulsion for $\chi_0 \sim 1$ and the energy minimum takes place at $R_m \sim \lambda_e$. Fig. (1) shows the energy of two vortices separated by a distance R . For $\chi_0 \sim 1$, the net interaction is attractive for large separations $\lambda_e < R < \Lambda$ and repulsive at short distances $R < \lambda_e$. There is also a long-range repulsion for $R > \Lambda$ due to the surface effect. Since the susceptibility χ_0 decreases with J_A , the attractive component drops as anisotropy increases. The inter-vortex interaction becomes purely repulsive for $\chi_0 \ll 1$.

Excitation of domain walls – We introduce the equation of motion for MMs and vortices that is used in the numerical simulation. The FM subsystem is described by the Landau-Lifshitz-Gilbert equation[21]

$$\partial_t \mathbf{m} = -\gamma \mathbf{m} \times \mathbf{B}_{\text{eff}} + \alpha \mathbf{m} \times \partial_t \mathbf{m}, \quad (9)$$

where γ is the gyromagnetic ratio, $\mathbf{m} = \mathbf{M}/M_s$ is the normalized MM, α is the damping coefficient and the effective

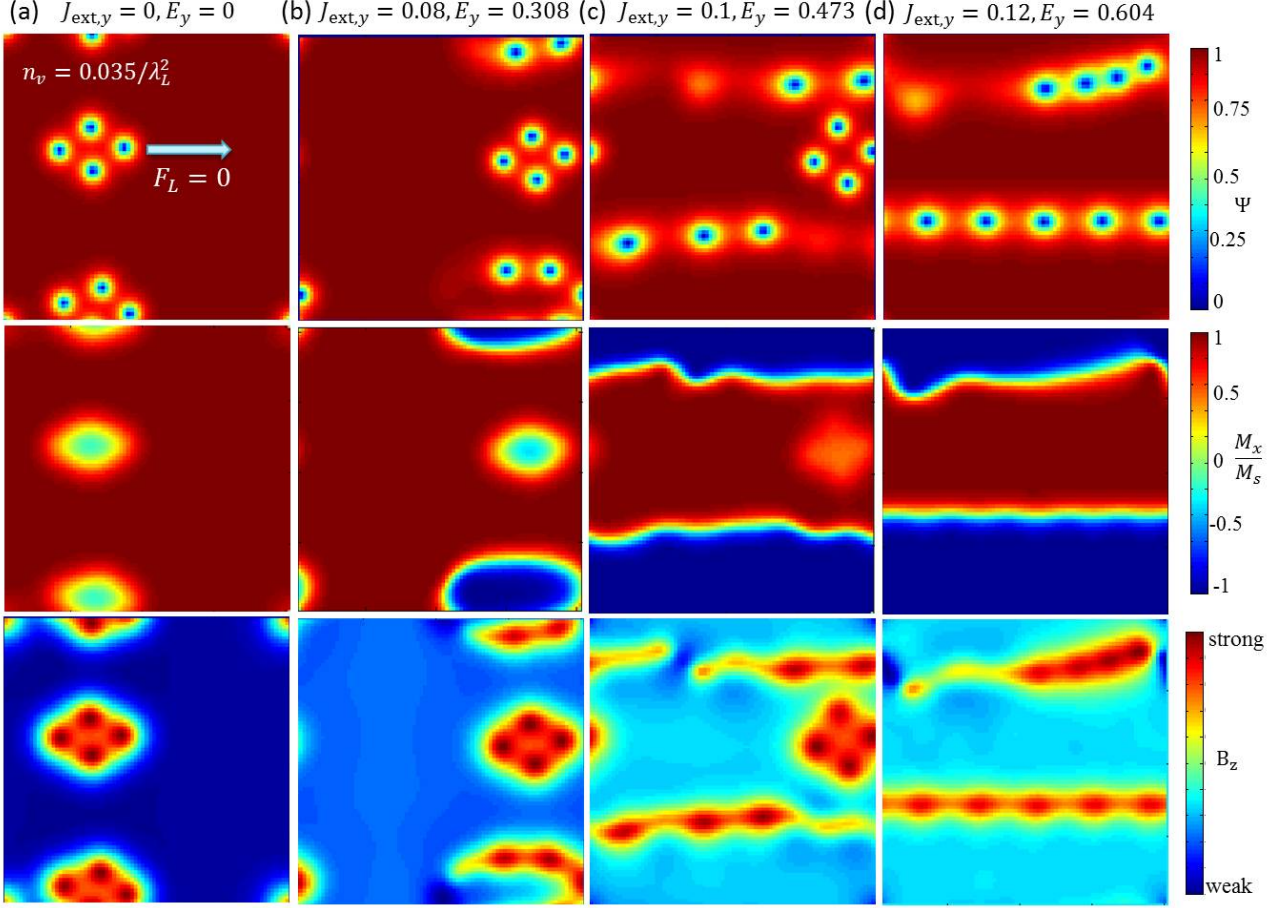


FIG. 2. (color online) (a-b): Development of the amplitude of superconducting order parameter $|\Psi|$, magnetic structure (x -component of the magnetic moment: M_x) and B_z as the current increases. The vortex positions correspond to the regions with suppressed $|\Psi|$. (a) Static configuration with $J_{\text{ext},y} = 0$. In (b-d), domain walls are created and the vortex configuration is modulated. $|\Psi|$ is suppressed (top row) and B_z is maximal (bottom row) in the normal core of vortices. MMs are canted by vortices so M_x is reduced (middle row).

magnetic field is $\mathbf{B}_{\text{eff}} = -\delta[g_M + g_{\text{int}}]/\delta\mathbf{M}$. The vortex subsystem is described by the time-dependent Ginzburg-Landau equations

$$\frac{\hbar^2}{2mD} \partial_t \Psi = - \left[\alpha_s \Psi + \beta |\Psi|^2 \Psi + \frac{\hbar^2}{2m} \left(i\nabla + \frac{2\pi}{\Phi_0} \mathbf{A} \right)^2 \Psi \right], \quad (10)$$

$$\frac{\sigma}{c} \partial_t \mathbf{A} = \mathbf{J}_s + \mathbf{J}_{\text{ext}} - \frac{c}{4\pi} \nabla \times (\nabla \times \mathbf{A} - 4\pi \mathbf{M}), \quad (11)$$

with the supercurrent

$$\mathbf{J}_s = \frac{e\hbar}{im} (\Psi^* \nabla \Psi - \Psi \nabla \Psi^*) - \frac{4e^2}{mc} |\Psi|^2 \mathbf{A}, \quad (12)$$

D is the diffusion coefficient, σ is the conductivity in the normal state, \mathbf{J}_{ext} is the external current and other parameters are defined according to the usual convention. The MMs stop responding to the vortex motion when the average magnetic field, $\bar{B}_z \approx n_v \Phi_0$ with n_v being the vortex density, is larger than the saturation value, $B_s = M_s J_A$, and the two subsystems

become decoupled. Therefore, we shall consider the interesting region $\bar{B}_z < B_s$.

In the long wavelength and weak damping $\alpha \ll 1$ limits, the magnon dispersion for the FM system of Eq.(9) is

$$\Omega^2 = \omega_0^2 + v_s^2 k^2, \quad v_s = \gamma M_s \sqrt{(2 - m_{z0}^2) J_A J}, \quad (13)$$

$$\omega_0^2 = J_A^2 \gamma^2 M_s^2 (1 - m_{z0}^2) \left[1 + i\alpha (2 - m_{z0}^2) (1 - m_{z0}^2)^{-1/2} \right], \quad (14)$$

where m_{z0} is the z component of the MMs in the ground state and v_s is the magnon velocity. $\text{Re}(\omega_0)$ is the energy gap and $\text{Im}(\omega_0)$ is the magnon relaxation rate. $\text{Re}(\omega_0) = 100$ GHz and $v_s = 50$ m/s for typical ferromagnets.[22]

We then establish general relations of the energy transfer between MMs and vortices. The vortex velocity acquires an ac part, $\tilde{\mathbf{v}}_i$, because of the interaction between vortices and MMs, $\mathbf{v}_i = \bar{\mathbf{v}} + \tilde{\mathbf{v}}_i$. The energy balance for the whole system reads

$$\eta \bar{v}^2 + \eta \langle \tilde{v}_i^2 \rangle_{i,t} + \frac{1}{n_v} \frac{\alpha}{M_s \gamma} \left\langle \int d\mathbf{r}^2 (\partial_t \mathbf{M})^2 \right\rangle_{x,t} = \mathbf{F}_L \cdot \bar{\mathbf{v}}, \quad (15)$$

where $\langle \dots \rangle_{i,t}$ denotes average over vortices and time, and $\langle \dots \rangle_{x,t}$ denotes average over space and time. The first and second term on the left-hand side (lhs) correspond to Bardeen-Stephen (BS) damping with coefficient $\eta = \Phi_0^2 \sigma / (2\pi c^2 \xi^2)$ [20], where $\xi = \sqrt{\hbar^2 / (2m|\alpha_s|)}$ is the coherence length. The third term on the lhs accounts for the dissipation due to precession of MMs. The term on the right-hand side is the work done by the Lorentz force F_L . The effective viscosity $\eta_{\text{eff}} = F_L / \bar{v}$ is enhanced due to the interaction between vortices and MMs,

$$\eta_{\text{eff}} = \eta + \frac{\eta}{\bar{v}^2} \langle \bar{v}_i^2 \rangle_{i,t} + \frac{1}{n_v \bar{v}^2} \frac{\alpha}{M_s \gamma} \left\langle \int dr^2 (\partial_t \mathbf{M})^2 \right\rangle_{x,t}. \quad (16)$$

Off resonance, the contribution of the magnetic damping is small, thus $\bar{v} \approx F_L / \eta$. Since $F_L = J_{\text{ext}} \Phi_0 / c$ and $E = \bar{v} n_v \Phi_0 / c$ with an external current J_{ext} and electric field E , the underlying dynamics can be probed by the I-V measurement.

The effect of magnons on the vortex dynamics depends on the vortex density. When the average inter-vortex distance is smaller than the value corresponding to the potential minimum, $n_v < 1/R_m^2$, the attraction between vortices dominates. Vortices form circular clusters with internal triangular structure in the ground state, as shown in Fig. 2 (a) obtained from our simulations[23]. The distance between neighboring vortices inside the cluster is of order λ_e , and the separation between neighboring clusters is of order $\sqrt{\pi R_c^2 / (n_v \lambda_c^2)}$, with a cluster radius given by $R_c \approx \Lambda[-u_a / (3u_r)]^{1/3}$. [24] The attractive, $u_a < 0$, and repulsive, $u_r > 0$, energies are defined in Fig. 1. The vortex clusters start to merge and more complex vortex configurations, such as stripes, are possible for larger values of n_v . The $H = H_{c1}$ transition from the uniform Meissner state to the state with vortex clusters is of first order [25–27] in contrast to the second order phase transition expected for conventional type II superconductors[20]. Vortex clusters in conventional superconductors with inter-vortex attraction, such as Nb, have been observed experimentally, see Ref. [28] for a review.

For finite transport current, each cluster driven by the Lorentz force moves as a whole and polarizes the MMs along its way. The MMs relax to their positions of equilibrium after the vortex cluster leaves that region. The polarization and excitation of magnons, and subsequent relaxation of MMs thus causes vortex dissipation through the magnetic subsystem[29]. The static structure of the vortex clusters remains the same for a small v because the change of the vortex-vortex interaction is negligible for $\xi_m / \lambda_e \ll 1$.

Here we derive a resonant condition between the motion of vortex clusters and magnon emission. The magnetic field distribution produced by the vortex motion has a dominant wave vector $G_x = 2\pi/R_m$, with $R_m \approx \lambda_e$ as shown in Fig. 1. The unperturbed ordered state has $M_{z0} = 0$. The resonant condition $G_x v = \Omega(G_x)$ gives a resonant velocity for vortices moving along the x direction

$$v_t = \gamma M_s \sqrt{2J_A J + \frac{R_m^2 J^2}{4\pi^2}}. \quad (17)$$

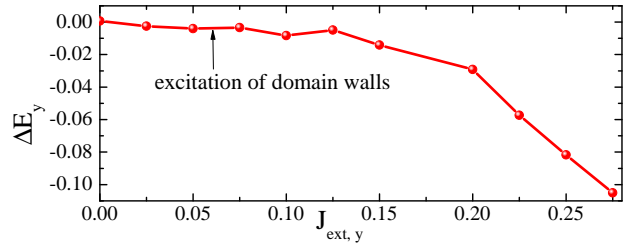


FIG. 3. (color online) Difference between the electric fields induced with and without magnetic moments as a function of current $J_{\text{ext},y}$, $\Delta E = E_M - E_B$, where E_M is the electric field for the system with magnetic moments and E_B is the electric field for the system without magnetic moments. The vortex viscosity increases when domain walls are created resulting in a drop of the electric field (vortex velocity).

This linear analysis is correct as long as the canted MMs satisfy the condition that $M_{zc} \approx \Phi_0 / (J_A R_m^2) \ll M_s$ [or $J_A \gg \Phi_0 / (R_m^2 M_s)$].

The oscillation amplitude of MMs and the ac part of the vortex velocity are greatly enhanced in resonance and η_{eff} increases according to Eq. (16). Two competing processes are involved in the magnetic subsystem: the energy input from vortex motion and the magnetic relaxation. For large dissipation ($\alpha \gg 1$), the excited magnon is quickly dissipated and the vortex cluster with canted MMs remains stable. On the contrary, the incoming energy accumulates for weak magnetic dissipation, $\alpha \ll 1$, and increases with time. This effect leads to an instability of the magnon excitations that has been discussed decades ago both experimentally [30] and theoretically[31–33]. For a large enough oscillation amplitude, the MMs are no longer restricted to one of the symmetry-breaking states (there are two degenerate ground states with $M_{x0} = \pm M_s \sqrt{1 - m_{z0}^2}$) and they can flip to the other ground state (with opposite M_{x0}). Domain walls are then created as shown in Fig. 2(b, c, d). M_z becomes large inside the domain walls and this effect increases the coupling between the magnetic subsystem and vortices. For $v \gg v_t$, the cluster structure evolves into vortex stripes along the driving direction [2(b, c, d)]. The domain walls are oriented along the vortex stripes due to the strong attraction between vortices and domain walls. Vortex stripes for large driving forces and random pinning potentials have also been observed in numerical simulations without MMs [34]. As vortex clusters drive domain walls, the dissipation increases and the vortex velocity (voltage) drops as shown in Fig. 3. The threshold velocity obtained from simulations where the domain walls are created is compatible with that estimated from Eq.(17).

Discussions – The magnetic susceptibility is small, $\chi_0 \ll 1$, in bulk FM superconductors such as UGe₂[35]. Thus, the attraction between vortices is negligible and the ground state is a triangular vortex lattice. In the flux flow regime, the vortex lattice is resonant with the oscillations of MMs when $\mathbf{G} \cdot \mathbf{v} = \Omega(\mathbf{G})$ is satisfied. We predict an enhancement of the

vortex viscosity at resonance, which can be probed by the I-V measurement. A large susceptibility, $\chi_0 \sim 1$, is needed to realize the vortex cluster configuration. This requirement can be fulfilled by some cuprate superconductors with rear-earth elements (Re), such as $\text{ReBa}_2\text{Cu}_3\text{O}_x$, where Re ions order antiferromagnetically below $T_N \sim 1$ K. Spins are free from the molecular field above the Neel temperature $T_N \sim 1$ K and can be easily polarized [36, 37] to mediate the attraction between vortices in the low magnetic field region. The vortex cluster phase can also be achieved in heterostructures of superconductors and ferromagnets with large susceptibility [38]. On the other hand, random pinning centers may prevent the formation of vortex clusters because pinning is strong for a small vortex densities. However, vortex motion in the flux flow regime quickly averages out the effect of random pinning centers [39, 40] and the cluster structure may be recovered.

Acknowledgement – We are indebted to V. Kogan, B. Maiorov, M. Weigand, C. J. Olson Reichhardt and C. Reichhardt for helpful discussions. The present work is supported by the Los Alamos Laboratory directed research and development program with project number 20110138ER.

-
- [1] L. N. Bulaevskii, A. I. Buzdin, M. L. Kubic, and S. V. Panjukov, *Adv. Phys.* **34**, 175 (1985).
- [2] S. S. Saxena, P. Agarwal, K. Ahilan, F. M. Grosche, R. K. W. Haselwimmer, M. J. Steiner, E. Pugh, I. R. Walker, S. R. Julian, P. Monthoux, G. G. Lonzarich, A. Huxley, I. Sheikin, D. Braithwaite, and J. Flouquet, *Nature* **406**, 587 (2000).
- [3] D. Aoki, A. Huxley, E. Ressouche, D. Braithwaite, J. Flouquet, J. P. Brison, E. Lhotel, and C. Paulsen, *Nature* **413**, 613 (2001).
- [4] C. Pfleiderer, M. Uhlarz, S. M. Hayden, R. Vollmer, H. v. Lohneysen, N. R. Bernhoeft, and G. G. Lonzarich, *Nature* **412**, 58 (2001).
- [5] P. C. Canfield, P. L. Gammel, and D. J. Bishop, *Phys. Today* **51**, 40 (1998).
- [6] J. H. Chu, J. G. Analytis, C. Kucharczyk, and I. R. Fisher, *Phys. Rev. B* **79**, 014506 (2009).
- [7] A. Buzdin, *Nature Mater.* **3**, 751 (2004).
- [8] I. F. Lyuksyutov and V. L. Pokrovsky, *Adv. Phys.* **54**, 67 (2005).
- [9] M. Tachiki, H. Matsumoto, T. Koyama, and H. Umezawa, *Solid State Commun.* **34**, 19 (1980).
- [10] L. N. Bulaevskii, E. M. Chudnovsky, and M. P. Maley, *Appl. Phys. Lett.* **76**, 2594 (2000).
- [11] A. Shekhter, L. N. Bulaevskii, and C. D. Batista, *Phys. Rev. Lett.* **106**, 037001 (2011).
- [12] L. N. Bulaevskii, M. Hruska, and M. P. Maley, *Phys. Rev. Lett.* **95**, 207002 (2005).
- [13] I. W. Sumarlin, S. Skanthakumar, J. W. Lynn, J. L. Peng, Z. Y. Li, W. Jiang, and R. L. Greene, *Phys. Rev. Lett.* **68**, 2228 (1992).
- [14] A. C. McLaughlin, W. Zhou, J. P. Attfield, A. N. Fitch, and J. L. Tallon, *Phys. Rev. B* **60**, 7512 (1999).
- [15] A. I. Buzdin, *Rev. Mod. Phys.* **77**, 935 (2005).
- [16] J. R. Kirtley, V. G. Kogan, J. R. Clem, and K. A. Moler, *Phys. Rev. B* **59**, 4343 (1999).
- [17] E. I. Blount and C. M. Varma, *Phys. Rev. Lett.* **42**, 1079 (1979).
- [18] J. Pearl, *Appl. Phys. Lett.* **5**, 65 (1964).
- [19] J. C. Wei and T. J. Yang, *Jpn. J. Appl. Phys.* **35**, 5696 (1996).
- [20] M. Tinkham, *Introduction to Superconductivity* (McGraw-Hill, Inc., New York, 1996).
- [21] T. L. Gilbert, *IEEE Trans. Magn.* **40**, 3443 (2004).
- [22] S. J. Pickart, H. A. Alperin, V. J. Minkiewicz, R. Nathans, G. Shirane, and O. Steinsvoll, *Phys. Rev.* **156**, 623 (1967).
- [23] For numerical purposes, length is in units of λ_L , time t is in units of ξ^2/D , conductivity σ is in units of $c^2\tau/(4\pi\lambda_L^2)$, the superconducting order parameter Ψ is in units of $\sqrt{|\alpha_s|/\beta}$, the magnetic field \mathbf{B} and magnetization \mathbf{M} are in units of $\Phi_0/(2\pi\xi^2\kappa)$, γ is in units of $2\pi\kappa D/\Phi_0$ and the exchange parameter J is in units of λ_L^2 . Here $\lambda_L = \sqrt{mc^2\beta/(16\pi|\alpha_s|e^2)}$ is the London penetration depth, $\xi = \sqrt{\hbar^2/(2m|\alpha_s|)}$ is the coherence length, $\kappa = \lambda_L/\xi$ is the Ginzburg-Landau parameter. The system is discretized into a mesh with size $0.2\lambda_L$. We use periodic boundary conditions [27]. Equation (9) is solved by an explicit numerical scheme developed in Ref. [41], and Eqs. (10) and (11) are solved by using the finite-difference method in Ref. [27]. We apply a current along the y direction, $J_{\text{ext},y}$ and calculate the electric field along the same direction $E_y = -\partial_t A_y$. The I-V curve is calculated with and without the magnetic subsystem to obtain the magnetic contribution to the voltage drop. The simulation parameters are: anisotropy parameter $J_A = 13$, saturation magnetization $M_s = 0.05$, exchange parameter $J = 4$, $\alpha = 0.01$, $\gamma = 0.5$, $\sigma = 1$ and $\kappa = 2$. The size of simulation box is $16\lambda_L \times 16\lambda_L \times 1\lambda_L$ and density of vortex is $n_v = 0.035/\lambda_L^2$.
- [24] See supplemental material at (xx).
- [25] M. Tachiki, H. Matsumoto, and H. Umezawa, *Phys. Rev. B* **20**, 1915 (1979).
- [26] A. I. Buzdin, S. S. Krotov, and D. A. Kuptsov, *Physica C* **175**, 42 (1991).
- [27] S. Z. Lin and X. Hu, *Phys. Rev. B* **84**, 214505 (2011).
- [28] E. H. Brandt, *Rep. Prog. Phys.* **58**, 1465 (1995).
- [29] L. N. Bulaevskii and S. Z. Lin, *Phys. Rev. Lett.* **109**, 027001 (2012).
- [30] N. Bloembergen and S. Wang, *Phys. Rev.* **93**, 72 (1954).
- [31] H. Suhl, *J. Phys. and Chem. Solids* **1**, 209 (1957).
- [32] E. Schlömann, *J. Appl. Phys.* **32**, 1006 (1961).
- [33] M. Chen and C. E. Patton, *Nonlinear Phenomena and Chaos in Magnetic Materials, Editor: P. E. Wigen* (World Scientific Pub. Co. Inc., Singapore, 1994).
- [34] C. Reichhardt, C. J. Olson Reichhardt, I. Martin, and A. R. Bishop, *Phys. Rev. Lett.* **90**, 026401 (2003).
- [35] A. D. Huxley, S. Raymond, and E. Ressouche, *Phys. Rev. Lett.* **91**, 207201 (2003).
- [36] P. H. Hor, R. L. Meng, Y. Q. Wang, L. Gao, Z. J. Huang, J. Bechtold, K. Forster, and C. W. Chu, *Phys. Rev. Lett.* **58**, 1891 (1987).
- [37] P. Allenspach, B. W. Lee, D. A. Gajewski, V. B. Barbeta, M. B. Maple, G. Nieva, S. I. Yoo, M. J. Kramer, R. W. McCallum, and L. Ben-Dor, *Z. Phys. B* **96**, 455 (1995).
- [38] Z. R. Yang, M. Lange, A. Volodin, R. Szymczak, and V. V. Moshchalkov, *Nature Mater.* **3**, 793 (2004).
- [39] A. E. Koshelev and V. M. Vinokur, *Phys. Rev. Lett.* **73**, 3580 (1994).
- [40] R. Besseling, N. Kokubo, and P. H. Kes, *Phys. Rev. Lett.* **91**, 177002 (2003).
- [41] C. Serpico, I. D. Mayergoyz, and G. Bertotti, *J. Appl. Phys.* **89**, 6991 (2001).

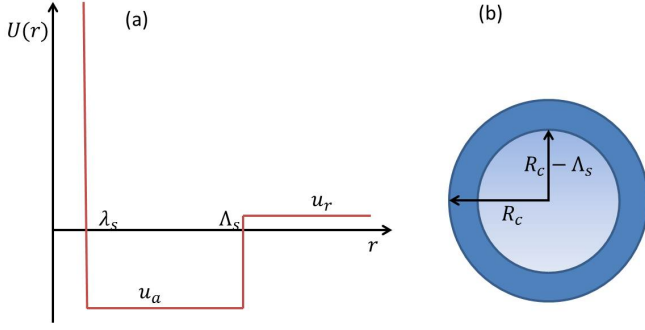


FIG. 4. (color online) (a) Approximated inter-vortex potential inside a vortex cluster. $\lambda_s \approx \lambda_e$ and $\Lambda_s = \Lambda$ compared with the interaction profile in Fig. 1 of the main text. (b) Partition of the vortex cluster with radius R_c to calculate the energy of the cluster.

Supplement : Characterization of the vortex cluster phase

Here we characterize the vortex cluster phase by using a simple model. The vortex clusters form a triangular lattice with lattice constant a_c . Each cluster contains n_c vortices. In the dilute vortex phase, the interaction between vortex clusters is Coulomb-like,

$$U_{cc} = \frac{\Phi_0^2 n_c^2}{4\pi^2} \sum_{i,j} \frac{1}{R_{c,i} - R_{c,j}}, \quad (18)$$

where $R_{c,i}$ is the position of the cluster and the summation is over all clusters. The summation is calculated numerically and the result is well approximated by the expression

$$U_{cc} \approx \frac{\Phi_0^2 n_c^2}{4\pi^2 a_c} (1.6N_c^{1.5} - 2N_c), \quad (19)$$

where N_c is the number of clusters. $N_c = n_v L^2 / n_c$ and $a_c = L / \sqrt{N_c}$ in a sample with lateral size L^2 and vortex density n_v . The repulsion between all clusters is

$$U_{cc} = -\frac{\Phi_0^2 n_v \sqrt{n_v} L^2}{2\pi^{3/2}} \frac{R_c}{\lambda_s} + 1.6 \frac{\Phi_0^2 (n_v L^2)^2}{4\pi^2 L}, \quad (20)$$

where we have used $N_c = n_v L^2 / (\pi R_c^2 / \lambda_s^2)$. R_c is the cluster radius and λ_s is the separation between two nearest vortices inside the cluster. The number of vortices in a cluster is $n_c =$

$\pi R_c^2 / \lambda_s^2$. Since the R_c -independent term of Eq.(20) is irrelevant in the following calculations, we will neglect it.

To estimate the interaction energy inside the cluster we approximate the inter-vortex interaction as shown in Fig. 4(a). A vortex in the region with radius $R_c - \Lambda_s$ attracts vortices in a region $\pi \Lambda_s^2$ and repels vortices in a region $\pi (R_c^2 - \Lambda_s^2)$ [see Fig. 4(b)]. Then, the interaction energy in the region with radius $R_c - \Lambda_s$ is

$$U_{c1} = \frac{\pi}{2\lambda_s^4} (R_c - \Lambda_s)^2 [\pi \Lambda_s^2 u_a + \pi (R_c^2 - \Lambda_s^2) u_r], \quad (21)$$

where $u_a < 0$ is the attraction and $u_r > 0$ is the repulsion. A vortex in the ring $R_c - \Lambda_s < r < R_c$ attracts less vortices. The attraction region for a vortex in the ring can be written as $\alpha' \Lambda_s^2$, with $\alpha' \approx 2$ obtained by direct integration over the ring area. The repulsion region is given by $\pi R_c^2 - \alpha' \Lambda_s^2$. The interaction energy in the ring is then given by

$$U_{c2} = \frac{\pi R_c}{\lambda_s^4} \Lambda_s [2\Lambda_s^2 u_a + (\pi R_c^2 - 2\Lambda_s^2) u_r]. \quad (22)$$

The total interaction in the vortex clusters is

$$U_c = N_c (U_{c1} + U_{c2}). \quad (23)$$

In thick superconductors with $d \gg \lambda$, we have $|u_a| \gg u_r$ and $R_c \gg \Lambda_s$. Then the energy of the whole system (apart from the R_c -independent contribution) is

$$U \approx -\frac{\Phi_0^2 n_v \sqrt{n_v} L^2}{2\pi^{3/2}} \frac{R_c}{\lambda_s} + \left(\frac{2\pi - \pi^2}{\lambda_s^4} R_c \Lambda_s^3 u_a + \frac{\pi^2}{2\lambda_s^4} R_c^4 u_r \right) \frac{n_v L^2 \lambda_s^2}{\pi R_c^2}, \quad (24)$$

where the first term accounts for the long-range repulsion between vortex clusters, and the second term accounts for the interaction inside clusters. The interaction between vortex clusters scales with the density as $n_v^{3/2}$ and the interaction inside the cluster scales as n_v . The first term can be neglected in the dilute vortex case $n_v \lambda_s^2 \ll 1$. By minimizing U with respect to R_c , we obtain the radius of the vortex cluster

$$R_c \approx \left(\frac{\pi - 2}{\pi} \frac{|u_a|}{u_r} \right)^{1/3} \Lambda_s, \quad (25)$$

and the distance between nearest vortex clusters is

$$a_c = \sqrt{\frac{\pi}{n_v}} \frac{R_c}{\lambda_s}. \quad (26)$$

By comparing the potential in Fig. 4(a) to the potential in Fig. 1 of the main text, we know that $\lambda_s \approx \lambda_e$ and $\Lambda_s \approx \Lambda$. Thus, we arrive to the results shown in the main text.